JOURNAL OF COMPUTATIONAL PHYSICS 86, 127–146 (1990)

A Numerical Study of the Nonlinear Schrödinger Equation Involving Quintic Terms

A. CLOOT, B. M. HERBST, AND J. A. C. WEIDEMAN

Department of Applied Mathematics, The University of the Orange Free State, P.O. Box 399, Bloemfontein 9300, South Africa

Received February 13, 1987; revised February 13, 1989

The cubic-quintic Schrödinger equation is known to possess solutions that grow unboundedly in finite time. By exploiting its conservation properties we derive sufficient conditions for bounded solutions. The computation of solutions near the critical threshold poses difficulties, since the number of active Fourier-components increase dramatically, resulting in steep temporal and spatial gradients. To overcome this difficulty we propose an efficient pseudospectral scheme which adaptively adjust the number of degrees of freedom.

1. INTRODUCTION

The cubic Schrödinger equation has attracted much attention from numerical analysts during the past couple of years, see, e.g., Weideman [12] and the references therein. This interest is in the first place due to the important role it has played in the development of soliton theory over the last twenty years. Newell [5] gives an up to date account of this.

In addition the equation has also proven to be a useful model problem for numerical analysts attempting to devise more efficient numerical methods for solving nonlinear dispersive wave problems in general. In particular, it has been demonstrated (Herbst *et al.*, [2], Sanz-Serna and Verwer [8]) that the equation becomes much harder to solve numerically if the contribution from the nonlinear part increases. This is caused by a spreading of the active wave numbers in Fourier space which is related to an increase in the spatial gradients in physical space.

In this paper we go one step further by increasing the order of the nonlinearity from cubic to quintic. It is well known, see, e.g., Glassey [1], that the solution in this case may become unbounded in finite time unless the initial condition is suitably restricted. Thyagaraja [11] related this to an unlimited spread of the active modes in Fourier space. His ideas, which are applied to the present situation in Section 2.3, enable us to conclude that the number of active modes in Fourier space will remain bounded provided a "smallness" condition is satisfied by the initial condition.

Since the number of active Fourier modes remains bounded, a spectral Fourier method should be particularly appropriate to solve the equation numerically as has

581/86/1-9

0021-9991/90 $3.00

been confirmed by several authors, see, e.g., Taha and Ablowitz [9]. This idea is exploited in the present paper by allowing the number of modes in our pseudo-spectral implementation to vary adaptively. This may result in considerable savings in computational cost in situations where the number of active Fourier modes may vary considerably during the course of the computation. One such situation occurs in the time evolution of the Benjamin–Feir side-band instabilities which will be discussed in detail.

Finally, we would like to comment briefly on the physical significance of the equation in the form used in this paper. It may be viewed as a model of the situation which arises when a multiple scales expansion of the Euler equations is taken to a higher order as the one from which the cubic Schrödinger equation results, see, e.g., Johnson [3], Kakutani and Michihiro [4]. However, we have ignored the important contribution from the nonlinear derivatives.

We have done extensive numerical experiments with the so-called derivative Schrödinger equation

$$iu_t + u_{xx} + iq(|u|^2)_x = 0, \tag{1.1}$$

and an analysis similar to that given in this paper will be reported elsewhere.

PART I

2. *Theoretical Aspects*

In this first part of the work we outline the main properties of the cubic-quintic nonlinear Schrödinger equation. It will be convenient to express this equation in operator form

$$u_t = i\mathscr{L}u + i\mathscr{N}(u)u \tag{2.1}$$

where

$$\mathscr{L}u := u_{xx} \tag{2.2a}$$

and

$$\mathscr{N}(u) := q_c|u|^2 + q_q|u|^4. \tag{2.2b}$$

We shall assume L-periodic boundary conditions throughout; that is,

$$u(x, t) = u(x + L, t), \qquad t > 0. \tag{2.3}$$

2.1. *Conservation Laws*

Only two of the conservation laws satisfied by (2.1) are of relevance to the present study. They are

$$\frac{dI}{dt} = 0 \tag{2.4a}$$

where

$$I = \int |u|^2 \, dx, \tag{2.4b}$$

and

$$\frac{dJ}{dt} = 0, \tag{2.5a}$$

where

$$J = \int (|u_x|^2 - \tfrac{1}{2} q_c |u|^4 - \tfrac{1}{3} q_q |u|^6) \, dx. \tag{2.5b}$$

Here, and henceforth, integration is over one space period unless stated otherwise. We refer to (2.4) as the conservation of energy, and to (2.5) as the conservation of the second quantity.

2.2. *Linearized Stability Analysis*

Equation (2.1) admits the wave train solution

$$u(x, t) = a \exp i(kx - \omega t), \tag{2.6}$$

provided the nonlinear dispersion relation

$$\omega = k^2 - q_c |a|^2 - q_q |a|^4 \tag{2.7}$$

is satisfied. We refer to a, k, and ω respectively as the amplitude, wave number, and frequency of (2.6).

We consider the stability of the solution (2.6), which we denote by u_0. This solution is perturbed to

$$u = u_0(1 + \varepsilon(x, t)), \tag{2.8}$$

where $\|\varepsilon\|_\infty^2 \ll 1$ and $\|\varepsilon\|_\infty = \max_x |\varepsilon(x, t)|$. Substitution of (2.8) into (2.1) gives, to the first order, the evolution equation for the perturbation

$$\varepsilon_t = i\varepsilon_{xx} - 2k\varepsilon_x + i(q_c |a|^2 + 2q_q |a|^4)(\varepsilon + \varepsilon^*) \tag{2.9}$$

with ε^* denoting the complex conjugate of ε.

Assuming that ε is L-periodic we express it as the Fourier series

$$\varepsilon(x, t) = \sum_{n=-\infty}^{\infty} \hat{\varepsilon}_n(t) \exp(i\mu_n x) \tag{2.10}$$

with wave numbers

$$\mu_n := \frac{2\pi n}{L}.$$

Replacing ε by its Fourier expansion in (2.9) we obtain the system of differential equations for the coefficients $\hat{\varepsilon}_n(t)$,

$$\frac{d}{dt}\begin{pmatrix}\hat{\varepsilon}_n\\ \hat{\varepsilon}^*_{-n}\end{pmatrix}=i\begin{pmatrix}Q-2k\mu_n-\mu_n^2 & Q\\ -Q & -Q-2k\mu_n+\mu_n^2\end{pmatrix}\begin{pmatrix}\hat{\varepsilon}_n\\ \hat{\varepsilon}^*_{-n}\end{pmatrix} \tag{2.11}$$

with

$$Q:=q_c|a|^2+2q_q|a|^4. \tag{2.12}$$

The eigenvalues of this system are

$$\lambda_n=-2ik\mu_n\pm\mu_n\sqrt{2Q-\mu_n^2}. \tag{2.13}$$

Hence we have exponential growth in $|\hat{\varepsilon}_{\pm n}|$, if the condition

$$\mu_n^2<2Q, \tag{2.14a}$$

i.e.,

$$\mu_n^2<2q_c|a|^2+4q_q|a|^4 \tag{2.14b}$$

is satisfied.

Obviously the condition (2.14) cannot be satisfied if q_c and q_q are both negative or zero. Otherwise the condition can be met depending on the amplitude of the initial solution. The long time evolution of this instability is the focus of our investigation.

In the purely cubic case ($q_q=0$), it is well known that the instability cannot grow unboundedly [11, 1]. Inclusion of the quintic term no longer guarantees a bounded solution, as was pointed out by Weinstein [13] and Thyagaraja [11]. We now derive some sufficient conditions for boundedness, by using similar arguments as the latter reference.

2.3. *Boundedness of the Solution*

To obtain condition for boundedness of the solution our point of departure is the conservation laws (2.4) and (2.5). Let I be given by (2.4b), and define

$$M=I^{-1}\int|u_x|^2\,dx. \tag{2.15}$$

If x_0 is defined by

$$|u(x_0,t)|=\min_x|u(x,t)|, \tag{2.16}$$

then we have the identity

$$u^2(x,t)=u^2(x_0,t)+2\int_{x_0}^{x}uu_x\,dx. \tag{2.17}$$

Using Schwartz's inequality we obtain

$$|u(x, t)|^2 \leqslant I(L^{-1} + 2M^{1/2}) \tag{2.18}$$

and

$$\int |u(x, t)|^4 \, dx \leqslant \|u(x, t)\|_\infty \int |u(x, t)|^2 \, dx$$

$$\leqslant I^2(L^{-1} + 2M^{1/2}). \tag{2.19}$$

Similarly

$$\int |u(x, t)|^6 \, dx \leqslant I^3(L^{-1} + 2M^{1/2})^2. \tag{2.20}$$

The implication of (2.18) is that if M is bounded, then $\|u\|_\infty$ is bounded. Accordingly we investigate the boundedness of M by distinguishing between four cases.

Case I. $q_c > 0$, $q_q > 0$. Inserting the inequalities (2.18)–(2.20) in the second conservation law, (2.5b), yields, after some rearrangement

$$I(1 - \tfrac{4}{3} q_q I^2) M - I^2(q_c + \tfrac{4}{3} q_q L^{-1} I) M^{1/2}$$

$$- [L^{-1} I^2(\tfrac{1}{2} q_c + \tfrac{1}{3} L^{-1} q_q I) + J] \leqslant 0. \tag{2.21}$$

This inequality ensures that M is bounded, provided that

$$\tfrac{4}{3} q_q I^2 < 1. \tag{2.22}$$

Case II. $q_c < 0$, $q_q < 0$. The bound

$$M \leqslant J/I \tag{2.23}$$

follows trivially from (2.5b) and (2.15).

Case III. $q_c > 0$, $q_q < 0$. Following the same procedure as in Case I we obtain an inequality similar to (2.21), but with $q_q = 0$. Hence we have an unconditionally bounded solution.

Case IV. $q_c < 0$, $q_q > 0$. An inequality similar to (2.21) is derived, but with $q_c = 0$. Accordingly the inequality (2.22) guarantees a bounded solution.

To summarize, when $q_q \leqslant 0$ (Cases II and III), a bounded solution for all time is guaranteed. If $q_q > 0$ (Cases I and IV) a bounded solution is ensured by the smallness condition (2.22). Note that this condition is sufficient, but not necessary. Our numerical experiments will examine the sharpness of the bound (2.22).

2.4. *Compatibility between Linear Instability and Boundedness*

Let us now investigate the conditions under which we linear instability of Section 2.2 remains bounded. The initial condition corresponding to (2.6) and (2.8) shows that

$$I = |a|^2 \int |1+\varepsilon|^2 \, dx \approx |a|^2 L. \tag{2.24}$$

Let us now reconsider the Cases I–IV of the previous section.

Case I. $q_c > 0, q_q > 0$. The smallness condition (2.22) and Eq. (2.24) yield a maximum value for $|a|^2$, namely,

$$(|a|^2)_{\max} < \frac{\sqrt{3}}{2\sqrt{q_q}\, L}. \tag{2.25}$$

According to (2.14), all modes n which satisfy

$$|a|^2 > \gamma_n \tag{2.26}$$

with

$$\gamma_n := \frac{-q_c + \sqrt{q_c^2 + 16 q_q \pi^2 n^2 L^{-2}}}{4q_q} \tag{2.27}$$

are linearly unstable. The following situations may be identified:

$0 < |a|^2 < \gamma_1$: no linear instability is possible

$\gamma_1 \leqslant |a|^2 < (|a|^2)_{\max}$: a bounded linear instability is possible

$(|a|^2)_{\max} < |a|^2$: the linear instability is not necessarily bounded.

Clearly if $|a|^2_{\max} < \gamma_1$ then a bounded linear instability cannot be ensured. This will be the case if

$$\frac{q_c}{\sqrt{q_q}} = \frac{4\pi^2 - 3}{\sqrt{3}\, L}. \tag{2.28}$$

Case II. $q_c < 0$, $q_q < 0$. No linear instability is admitted and the solution remains bounded for all time.

Case III. $q_c > 0$, $q_q < 0$. There is a bounded linear instability in all modes n which satisfy (2.14). Hence, necessary conditions for instability are

$$|q_q| < q_c^2 L^2/(16\pi^2) \tag{2.29a}$$

and

$$|a|^2 \in (R_-, R_+), \qquad \text{where} \quad R_\pm := (q_c \pm \sqrt{q_c^2 - 16|q_q|\pi^2/L^2})/(4|q_q|). \tag{2.29b}$$

Case IV. $q_c \leqslant 0$, $q_c > 0$. Reasoning similar to that leading to (2.28) shows that in this case we need simultaneously

$$|a|^4 > \pi^4/q_q L^2$$

and

$$|a|^4 < \frac{3}{4}\frac{1}{q_q L^2}.$$

This can obviously not be realised and a bounded solution cannot be guaranteed.

PART II

3. *Numerical Aspects*

3.1. *Introduction*

Before we describe the numerical methods, we introduce the following notation: The space interval $[-\frac{1}{2}L, \frac{1}{2}L]$ is descretized by the uniform N-grid

$$x_j := jh, \qquad j = -\tfrac{1}{2}N, \ldots, \tfrac{1}{2}N, \tag{3.1}$$

where the grid spacing is given by

$$h := L/N. \tag{3.2}$$

Let $U_j(t)$ denotes the approximate solution to $u(x_j, t)$. The discrete Fourier transform of the discrete function $\{U_j\}$ is defined as

$$F_n U_j := \hat{U}_n = \frac{1}{N}\sum_j U_j \exp(-i\mu_n x_j), \qquad n = -\tfrac{1}{2}N, \ldots, \tfrac{1}{2}N - 1 \tag{3.3}$$

with inverse formula

$$F_j^{-1}\hat{U}_n := U_j = \sum_n \hat{U}_n \exp(i\mu_n x_j), \qquad j = -\tfrac{1}{2}N, \ldots, \tfrac{1}{2}N - 1, \tag{3.4}$$

where μ_n is defined by (2.11). Here, and henceforth, summation indices range over $-\frac{1}{2}N$ to $\frac{1}{2}N - 1$. N is taken to be an even integer throughout.

3.2. *Space Discretization*

Our numerical method is based on the following pseudospectral space-discretization of (2.1)

$$\dot{U}_j = -iF_j^{-1}(\mu_n^2 F_n U_j) + \mathcal{N}(U_j), \tag{3.5}$$

where the "$\cdot$" denotes differentiation with respect to time, and

$$\mathcal{N}(U_j) := i(q_c|U_j|^2 + q_q|U_j|^4)\, U_j. \tag{3.6}$$

For the purely cubic case, ($q_q = 0$), the properties of the semi-discretization are discussed in Weideman [12]. These results are trivially extended to the quantic-cubic, and we merely list the relevant features:

— The discretization (3.5) conserves discrete analogues of both the conservation laws (2.4) and (2.5).

— The scheme (3.5) possesses the exact nonlinear dispersion relation (2.7), as well as the linear instability region (2.14) of the low wave numbers.

— Aliasing contributions are introduced by the scheme (3.5). These may be eliminated by either a dealiasing procedure [6, 7, 12] or by selecting N sufficiently large [12]. In the present study we shall opt for the latter course, by adapting the number of degrees of freedom automatically to ensure that we cover at all times all effective modes.

3.3. *Time Integration*

The results of Taha and Ablowitz [9] and Weideman [12] suggest that the most efficient time integration scheme for the system of ODEs (3.5), is the split-step method of Tappert [10]. This scheme is defined by the following steps:

1. First a so-called intermediate solution is computed by advancing the solution according to the exact solution of the purely nonlinear equation $u_t = \mathcal{N}(u)$, namely,

$$V_j^m = U_j^m \exp(iq\tau \mathcal{N}(U_j)). \tag{3.7a}$$

Here τ is the time step and U_j^m denotes the approximation to $u(x_j, m\tau)$.

2. The solution is advanced in Fourier space according to the linear dispersive equation $u_t = \mathcal{L}u$, namely,

$$\hat{V}_n^m = \frac{1}{N} \sum_j V_j^m \exp(-i\mu_n x_j) \tag{3.7b}$$

$$\hat{U}_n^{m+1} = \exp(-i\mu_n^2 \tau)\, \hat{V}_n^m \tag{3.7c}$$

$$U_j^{m+1} = \sum_n \hat{U}_m \exp(i\mu_n x_j). \tag{3.7d}$$

We also list the features of the scheme (3.7)

— The method is first-order accurate in time.

— The method conserves a discrete analogue of the energy (2.4), but not the second quantity (2.5).

— It possesses a nonlinear dispersion relation identical to (2.7).

— The method has the following step-size restrictions for an appropriate linearisation,

$$\tau < \frac{h^2}{\pi} \quad \text{if} \quad q_c|a|^2 + 2q_q|a|^4 > 0 \tag{3.8}$$

$$\frac{\tau}{2\theta + \pi} < \frac{h^2}{\pi^2} \quad \text{if} \quad q_c|a|^2 + 2q_q|a|^4 < 0, \tag{3.8b}$$

where $\theta = -\arccos 1/\sqrt{1 + (q_c|a|^2 + 2q_q|a|^4)^2\tau^2}$.

— Provided the step-size restrictions (3.8) are satisfied, the second quantity (2.5) turns out approximately constant during practical computations.

Since our numerical experiments are aimed at investigating near singular behaviour, it is enefficient to keep the number of degrees of freedom fixed. For an updating of the grid, we propose the following algorithm:

To obtain the initial number of degrees of freedom, we compute the Fourier transform $\hat{U}_n(0)$ of the initial condition. Let ε be a pre-assigned tolerance. Now N is selected such that

$$|\hat{U}_n| < \varepsilon \tag{3.9}$$

for all n such that $-\frac{1}{2}N \leqslant n \leqslant -\frac{1}{2}N + K$, $\frac{1}{2}N - K \leqslant n \leqslant \frac{1}{2}N$, where K is specified in advance. In other words, we require that the energy content of the $2K$ high wave numbers be sufficiently small.

Next the solution at the first time level is calculated according to the split-step scheme (3.7). If the criterion (3.9) is no longer valid (i.e., energy has flowed to some of the $2K$ high wave numbers) we return to the previous time level (step failed), and double the number of degrees of freedom. The function values at half-integer nodes are inexpensively calculated through discrete trigonometric interpolation. This procedure is applied until the criterion (3.9) is valid (step accepted).

On the other hand, if the criterion (3.9) is valid at the first step, it is checked whether the number of degrees of freedom can with safety be reduced by a factor one-half. This procedure is applied at each time level.

Of course, the time-step also needs updating to ensure that the linear instability condition (3.8) remains satisfied. For this purpose we let

$$\tau = \alpha \frac{h^2}{\pi}, \qquad \tau < \tau_{\max},$$

where $\tau_{\max}$ and $\alpha < 1$ are safety factors to be specified by the user.

We discuss some features of the above algorithm:

— Provided K is selected sufficiently large and ε is sufficiently small, we have very high accuracy in space. Also, the need for dealiasing has been circumvented. Moreover, the process is automatic.

— Provided N is selected to be a power of two initially, it remains so for all time. Hence the efficiency of the FFT is exploited to its fullest.

— Because N is doubled at each step the updating of the grid is inexpensive. Moreover, this procedure ensures that updating does not occur too frequently. Whenever two successive step failures occur, it is usually an indication that a singularity has been reached.

4. Numerical Experiments

In this section the algorithm described in Section 3.3 is used to solve (2.1) numerically. In all the experiments the initial condition

$$u(x, 0) = a(1 + \varepsilon \cos \mu x),$$

where

$$\mu = 2\pi/L$$

was used. The values of L, ε, and K are fixed at $L = 12$, $\varepsilon = 0.1$, and $K = 5$. We now proceed to describe the numerical experiments for different values of q_c, q_q, and a.

4.1. *Case* I. $q_c > 0$, $q_q > 0$

We recall from (2.28) that the bounded linear instability cannot be guaranteed if

$$q_c < \frac{4\pi^2 - 3}{\sqrt{3}\, L} \sqrt{q_q} \tag{4.1a}$$

or with $L = 12$,

$$q_c < 1.76\sqrt{q_q}. \tag{4.1b}$$

Since the evolution of the linear instability is under investigation the choice $q_c = 2$, $q_q = 0.25$ is appropriate. According to (2.25) and (2.27) the following behaviour is expected from different choices of $|a|$:

$0 < |a| < 0.2596$—no instability

$0.2596 < |a| < 0.3799$—a bounded linear instability

$0.3799 < |a| < \infty$—an unbounded nonlinear instability.

Figures 1a and 1b show the solution with an initial amplitude of $a = 0.35$ and the solution clearly displays recurrence, see, e.g., Yuen and Ferguson [14]. It may be argued that the subsequent development of the instability causes the amplitude to exceed the critical value of 0.3799 and, hence, should become unbounded if our bounds are sharp. However, it should be borne in mind that the smallness condition pertains to the initial condition and the solution preserves its "memory" of this condition through the conservation laws.

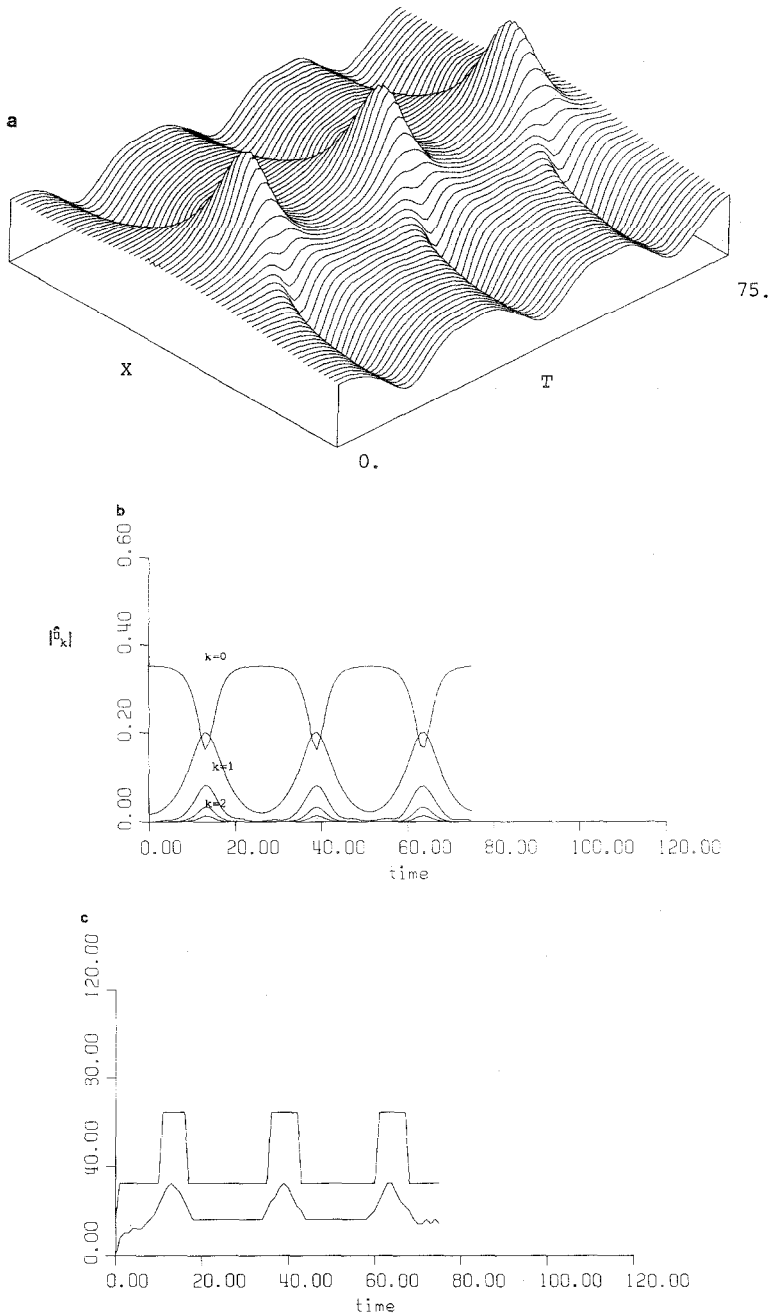

FIG. 1. Recurrence obtained from $q_c = 2$, $q_q = 0.25$, and $a = 0.35$: (a) The solution in physical space. (b) The Fourier representation. (c) A comparison between the number of active analytical modes and the number of modes included in the numerical scheme.

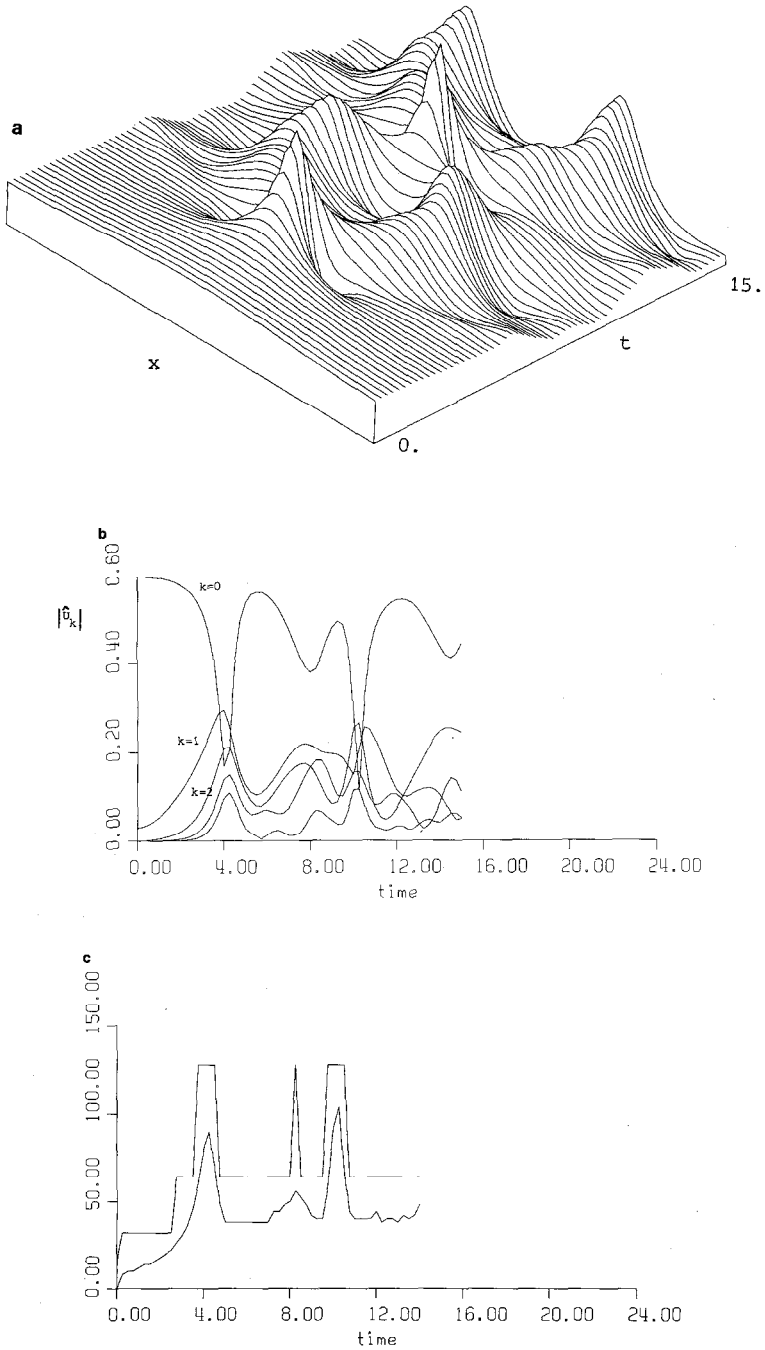

FIG. 2. A bounded instability obtained from $q_c = 2$, $q_q = 0.25$, and $a = 0.6$: (a), (b), and (c) as in Fig. 1.

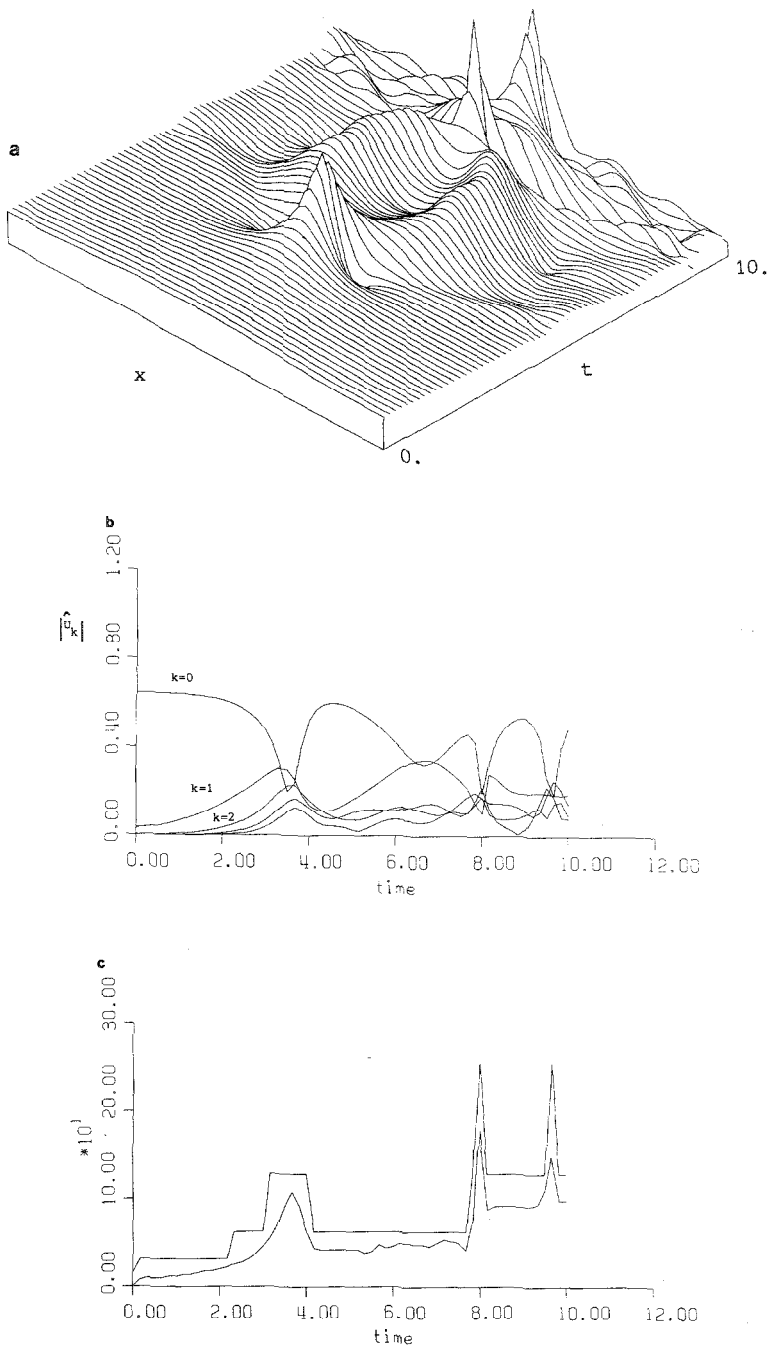

FIG. 3. An increasingly unstable solution obtained from $q_c = 2$, $q_q = 0.25$, and $a = 0.645$: (a), (b), and (c) as in Fig. 1.

Increasing the value of a to 0.6 (Fig. 2) and 0.645 (Fig. 3) shows the increasingly unstable behaviour of the solution. Starting with well-defined recurrence, we end up with solutions which become unbounded, with Fig. 3 falling on the edge between bounded and unbounded solutions.

The nature of the unstable behaviour may be observed from Figs. 1b, 2b, and 3b, which show that an increasing number of Fourier modes become activated.

The behavior of the algorithm is monitored in Figs. 1c, 2c, and 3c which show the number of Fourier modes included in our computations as well as the number of modes for which $|\hat{U}_n| > 10^{-6}$.

Although we have not tried for optimal efficiency, the computational cost of the adaptive scheme to calculate the solution of Fig. 3 is only about 15% of the cost of the fixed mode scheme, which in this case requires 256 modes.

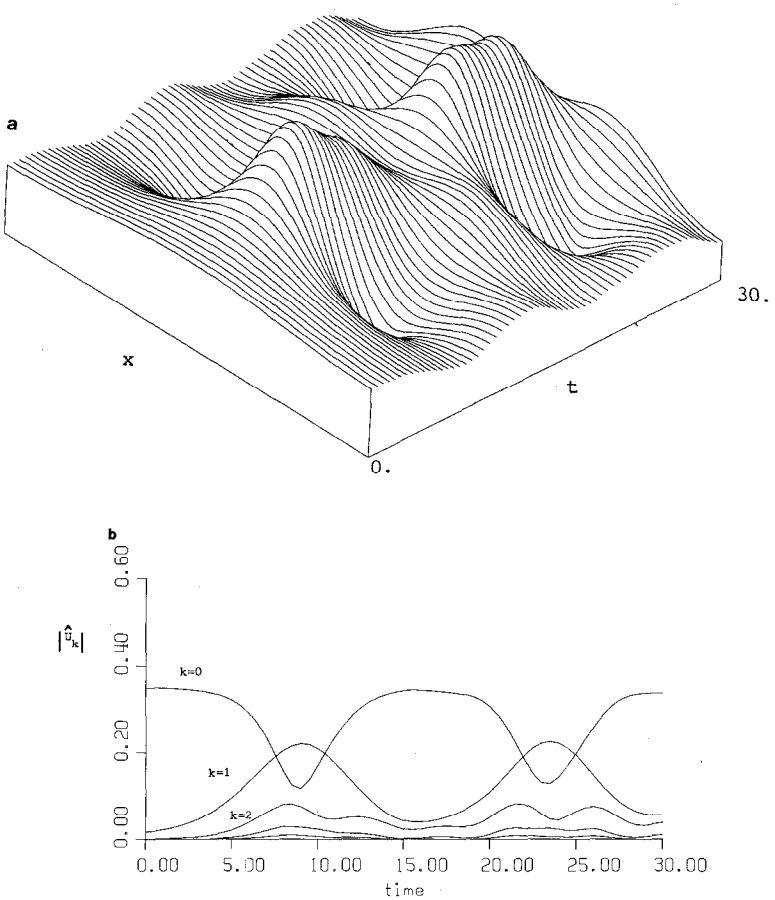

FIG. 4. Recurrence obtained from $q_c = 4$, $q_q = -3$, and $a = 0.35$: (a) The solution in physical space. (b) The Fourier representation.

4.2. *Case* III: $q_c > 0$, $q_q < 0$

According to the analysis of Section 2.4 this choice of the parameters leads to a bounded linear instability provided (2.2a) is satisfied. Choosing $q_c = 4$ and $q_q = -3$, (2.29a) is satisfied and (2.29b) becomes

$$a \in (0.190, 0.794).$$

Figures 4, 5, and 6 show the solutions with $a = 0.35$, $a = 0.49$, and $a = 0.74$, respectively. According to (2.14) these correspond to 1, 2, and 1 unstable modes, respectively. The behaviour of these unstable modes is best illustrated by Figs. 4b, 5b, and 6b.

4.3. *Case* IV: $q_c < 0$, $q_q > 0$

For this choice of the parameters, a bounded linear instability cannot be guaranteed and indeed, Fig. 7 shows that the solution becomes unbounded in finite time.

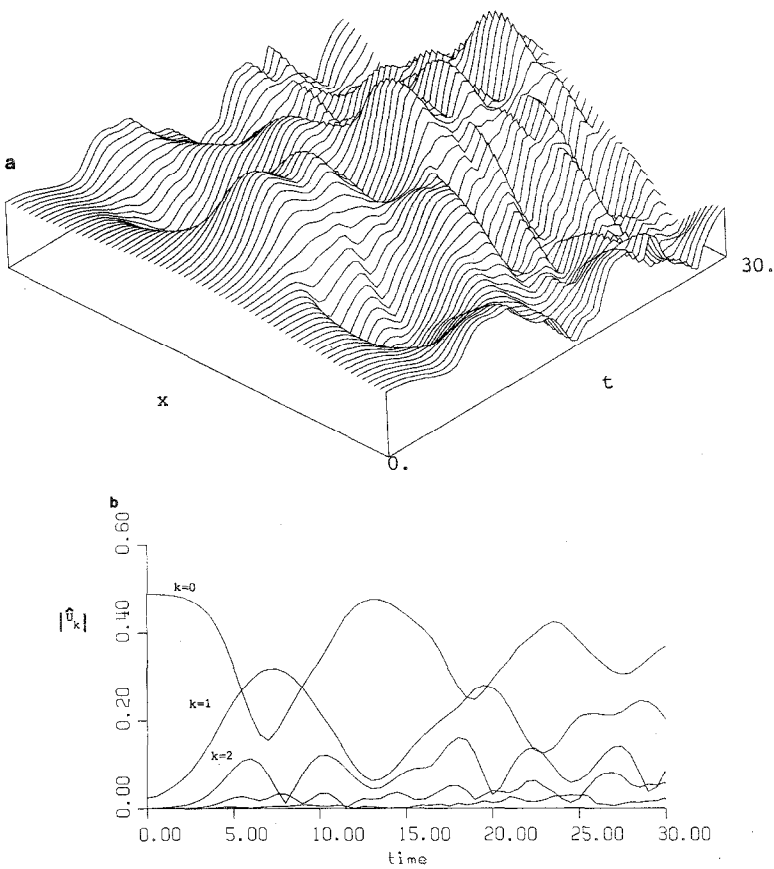

FIG. 5. A bounded unstable solution obtained from $q_c = 4$, $q_q = -3$, and $a = 0.49$: (a) and (b) as in Fig. 4.

Since the energy or L_2 norm remains constant the unbounded solution assumes the form of a delta function. Figure 7b again shows the number of modes allowed for in the computation as well as the actual number of non-zero modes. Accordingly, the blowup of the solution is identified with an unlimited growth in the number of non-zero Fourier modes.

The question now arises whether the bounds derived in this paper are sharp. Our numerical experiments indicate that the bound (2.14), pertaining to the linearized instability, is sharp. This has also been confirmed elsewhere in the case of a cubic nonlinearity, see, e.g., Weideman [12]. The situation with regard to the smallness condition (2.22) is less clear.

In Figs. 2 and 3 we have used values well outside the range where a bounded solution can be guaranteed and yet Fig. 2 gives no indication of a blowup. Of course, it is possible that a blowup may occur at a later time. However, the fact that

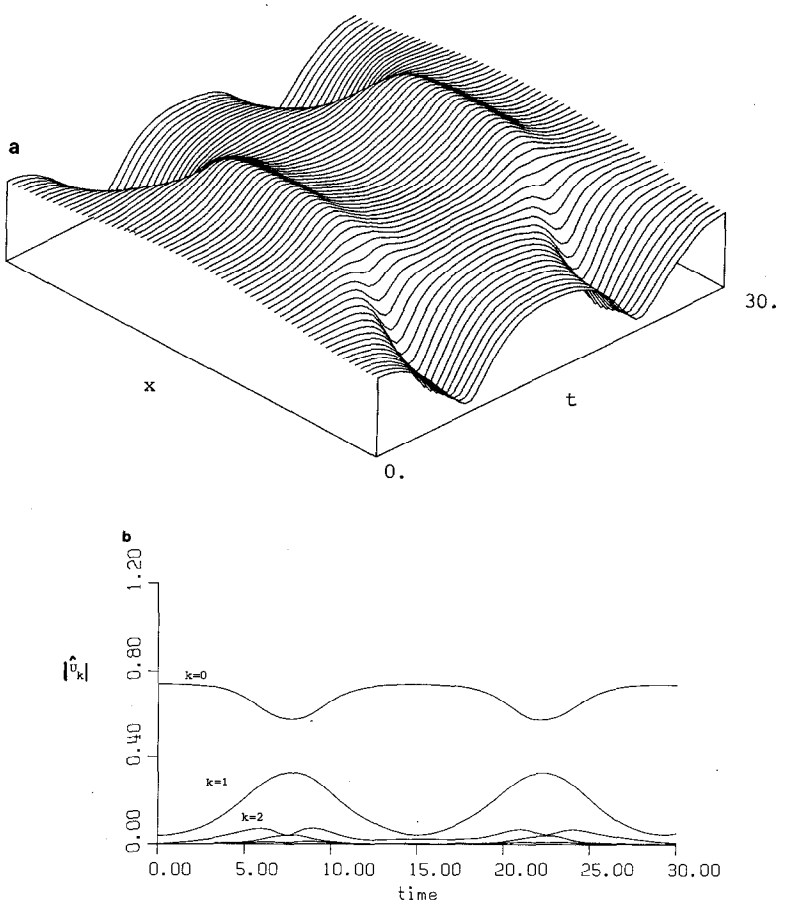

FIG. 6. Recurrence obtained from $q_c = 4$, $q_q = -3$, and $a = 0.74$: (a) and (b) as in Fig. 4.

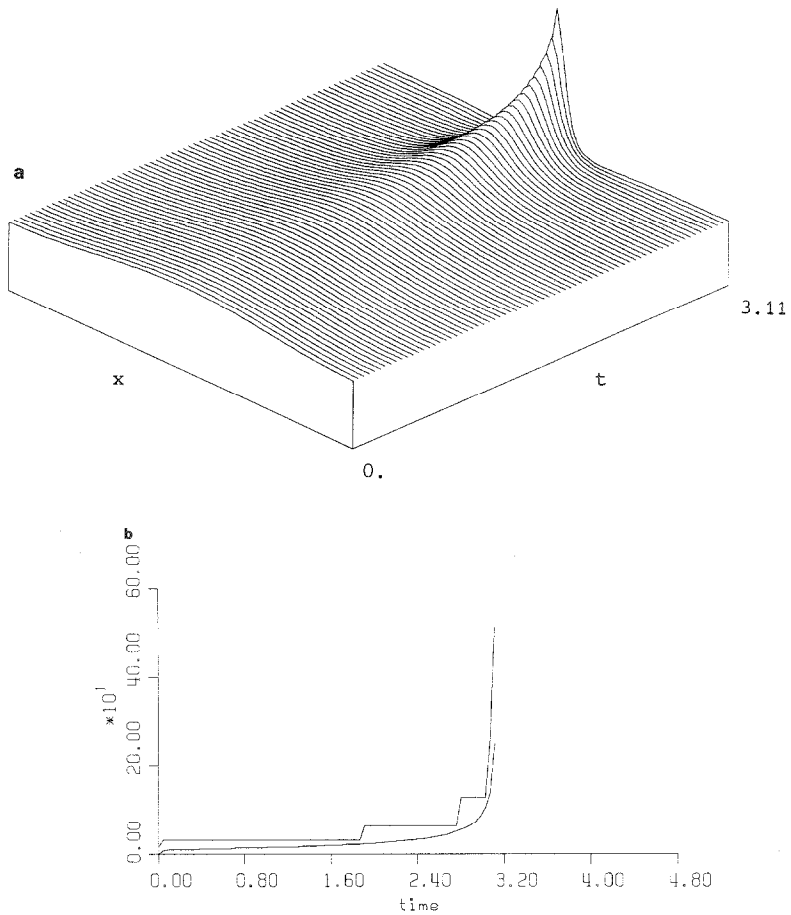

FIG. 7. A bounded unstable solution from $q_c = -1$, $q_q = 3$, and $a = 0.65$: (a) Physical space. (b) A comparison between the number of active analytical modes and the number of modes include in the numerical scheme.

the smallness condition (2.22) was obtained taking only two conservation laws into account as well as the roughness of some of the estimates, in our opinion, renders a sharp bound rather unlikely.

APPENDIX: A SMALLNESS CONDITION FOR A FINITE DIFFERENCE SCHEME

A smallness condition for the pseudospectral scheme follows in exactly the same way as (2.22) was obtained. We present the corresponding analysis for a finite difference scheme.

Consider the following discrete version of (2.1) and (2.2)

$$\dot{U}_j = i\mathscr{L}_h U_j + i\mathscr{N}(U_j)\, U_j, \tag{A.1}$$

where $\dot{U}_j$ denotes the time derivative of U_j,

$$\mathscr{L}_h U_j := (U_{j+1} - 2U_j + U_{j-1})/h^2 \tag{A.2}$$

and

$$\mathscr{N}(U_j) := q_c |U_j|^2 + q_q |U_j|^4. \tag{A.3}$$

If periodic boundary conditions

$$U_{-n/2} = U_{N/2}; \qquad U_{-(N+1)/2} = U_{(n+1)/2}$$

are used, it may be shown that

$$h \sum_{j=-N/2}^{(N-1)/2} |U_j|^2 = I \tag{A.4}$$

and

$$Nh \sum_{n=-N/2}^{(N-1)/2} \mu_n^2 |\hat{U}_n|^2 = \left(\frac{1}{2} q_c h \sum_{j=-N/2}^{(N-1)/2} |U_j|^4 + \frac{1}{3} h q_q h \sum_{j=-N/2}^{(N-1)/2} |U_j|^6 \right) = J \tag{A.5}$$

are constants in time. The $\hat{U}_n$ are given by (3.3).

Proceeding as in Section 2.3, we define

$$MI := h \sum_{j=-N/2}^{N/2} |(U_{j+1} - U_j)/h|^2$$

and choose s such that

$$|U_s| \leqslant |U_j| \qquad \text{for all } j.$$

After some manipulation, where use is made of the Schwartz inequality, it follows that

$$h \sum_j |U_j|^4 \leqslant I^2 \left(\frac{1}{L} + 2M^{1/2} \left(1 + hM^{1/2} + \frac{1}{4} h^2 M \right)^{1/2} \right) \tag{A.6}$$

and

$$h \sum_j |U_j|^6 \leqslant I^3 \left(\frac{1}{L} + 2L^{1/2} \left(1 + hM^{1/2} + \frac{1}{4} h^2 M \right)^{1/2} \right)^2. \tag{A.7}$$

From these expressions a bound for $L\sum_n \mu_n^2|\hat{U}_n|^2$ may be derived. Since

$$U_{j+1}-U_j=\sum_n \hat{U}_n \exp(i\mu_n x_j)(\exp(i\mu_n h)-1),$$

it follows that

$$IM = L\sum_n |\hat{U}_n|^2 \,|\exp(i\mu_n h)-1|^2/h^2.$$

The identity

$$\exp(x)-\exp(y)=(x-y)\int_0^1 \exp(sx+(1-s)\,y)\,ds$$

yields

$$|(\exp(i\mu_n h)-1)/h| \leqslant \mu_n.$$

Hence,

$$IM \leqslant L\sum_n \mu_n^2|\hat{U}_n|^2. \tag{A.8}$$

Defining

$$I\tilde{M} := L\sum_n \mu_n^2|\hat{U}_n|^2, \tag{A.9}$$

it follows from (A.5), (A.6), and (A.7) that

$$I\tilde{M} \leqslant J+\frac{1}{2}q_c I^2\left(\frac{1}{L}+2\tilde{M}^{1/2}\left(1+h\tilde{M}^{1/2}+\frac{1}{4}h^2\tilde{M}\right)^{1/2}\right)$$
$$+\frac{1}{3}q_q I^3\left(\frac{1}{L}+2\tilde{M}^{1/2}\left(1+h\tilde{M}^{1/2}+\frac{1}{4}h^2\tilde{M}\right)^{1/2}\right)^2. \tag{A.10}$$

In the limit $h\to 0$, this goes over into (2.21).

Althoug a complete analysis of (A.10) will not be attempted here, it is easy to show that $\tilde{M}$ will be bounded provided h is small enough. Also the smallness condition relating to (2.22) is to $O(h)$,

$$\tfrac{4}{3}q_q I^2+(\tfrac{1}{2}q_c I+\tfrac{2}{3}L^{-1}q_q I^2)h<1. \tag{A.11}$$

These results show that the solution of the difference scheme will remain bounded as $h\to 0$, provided the initial conditions are suitably restricted.

ACKNOWLEDGMENTS

We are grateful to Professor J. Ll. Morris who has generously shared his ideas with us during the early stages of this investigation. We are also pleased to acknowledge the financial support of the C.S.I.R., Pretoria.

REFERENCES

1. R. T. GLASSEY, *J. Math. Phys.* **18**, 1794 (1977).
2. B. M. HERBST, J. LL. MORRIS, AND A. R. MITCHELL, *J. Comput. Phys.* **60**, 282 (1985).
3. R. S. JOHNSON, *Proc. Roy. Soc. London Ser. A* **357**, 131 (1977).
4. T. KAKUTANI AND K. MICHIHIRO, *J. Phys. Soc. Japan* **52**, 4129 (1983).
5. A. C. NEWELL, *Solitons in Mathematics and Physics* Regional Conference Series in Applied Mathematics No. 48 (SIAM, CBMS-NSF, Philadelphia, 1985).
6. G. S. PATTERSON AND S. A. ORSZAG, *Phys. Fluids* **14**, 2538 (1971).
7. Y. SALU AND G. KNORR, *J. Comput. Phys.* **17**, 68 (1975).
8. J. M. SANZ-SERNA AND J. G. VERWER, *IMA J. Numer. Anal.* **6**, 25 (1986).
9. T. R. TAHA AND M. J. ABLOWITZ, *J. Comput. Phys.* **55**, 203 (1984).
10. T. R. TAHA AND M. J. ABLOWITZ, *J. Comput. Phys.* **55**, 203 (1984).
10. F. D. TAPPERT, *Lecture in Appl. Math.*, Vol. 15, p. 215 (Amer. Math. Soc., Cambridge, MA, 1974).
11. A. THYAGARAJA, "Recurrence Phenomena and the Number of Effective Degrees of Freedom in Nonlinear Wave motions, in *Nonlinear Waves*, edited by L. Debnath, Chap. 17, (Cambridge Univ. Press, London, 1983).
12. J. A. C. WEIDEMAN, Ph.D. thesis, Dept. Applied Mathematics, University of the Orange Free State, Bloemfontein, 1986 (unpublished).
13. WEINSTEIN, Ph.D. thesis, New York University, 1982.
14. H. C. YUEN AND W. E. FERGUSON, *Phys. Fluids* **21**, 1275 (1978).